E11839

STRUCTURE OF THE SOOT GROWTH REGION OF LAMINAR PREMIXED METHANE/OXYGEN FLAMES

F. Xu and G.M. Faeth*
Department of Aerospace Engineering
The University of Michigan
Ann Arbor, MI 48109-2140, U.S.A.

Introduction. Soot is a dominant feature of hydrocarbon/air flames, affecting their reaction mechanisms and structure. As a result, soot processes affect capabilities for computational combustion as well as predictions of flame radiation and pollution emissions. Motivated by these observations, the present investigation extended past work on soot growth in laminar premixed flames [1,2], seeking to evaluate model predictions of flame structure.

Xu et al. [1,2] report direct measurements of soot residence times, soot concentrations, soot structure, gas temperatures and gas compositions for premixed flames similar to those studied by Harris and Weiner [3] and Ramer et al. [4] respectively. It was found that predictions of major stable gas species concentrations based on mechanisms of Leung and Lindstedt [5] and Frenklach and coworkers [6-8], were in good agreement with the measurements. The results were also used to evaluate the hydrogen-abstraction/carbon-addition (HACA) soot growth mechanisms of Frenklach and coworkers [6-8] and Colket and Hall [9]. It was found that these mechanisms were effective using quite reasonable correlations for the steric factors appearing in the theories [1,2].

The successful evaluation of the HACA mechanism of soot growth in Refs. 1 and 2 is encouraging but one aspect of this evaluation is a concern. In particular, H-atom concentrations play a crucial role in the HACA mechanism and it was necessary to estimate these concentrations because they were not measured directly. These estimates were made assuming local thermodynamic equilibrium between H_2 and H based on measured temperatures and H_2 concentrations and the equilibrium constant data of Kee et al. [10]. This approach was justified by the flame structure predictions; nevertheless, direct evaluation of equilibrium estimates of H-atom concentrations in the soot growth regions of laminar premixed flames is needed to provide more convincing proof of this behavior. Thus, the objective of the present investigation was to complete new measurements of the structure of the soot growth region of laminar premixed flames and to use these results to evaluate whether H and H_2 are in thermodynamic equilibrium and to extend the earlier evaluation of predictions of concentrations of major gas species.

Experimental Methods. Measurements of H-atom concentrations in the premixed flames were carried out using the lithium chloride technique described by Neoh et al.[11]; this required the presence of lithium chloride particles in the reactant mixture so that the porous plate burner used in Ref. 1 and 2 could no longer be used because it trapped the particles. Thus, present measurements were carried out using a new burner with the test flames attached to a honeycomb element at the burner exit. Nitrogen coflow around the flames was used to eliminate the diffusion flames at the periphery of the hot fuel-rich mixture in the post flame region where soot growth occurs. The soot reaction region was stabilized by impinging the flame on a flat plate having a hole at the axis located 35 mm above the burner exit. The flames were also surrounded by screens and a plastic enclosure to control room disturbances. Measurements included soot volume fractions by deconvoluted laser extinction, soot temperatures by deconvoluted multiline emission, concentrations of major stable gas species by sampling and gas chromatography, concentrations of H by deconvoluted absorption based on the lithium chloride technique and gas velocities by laser velocimetry.

Computational Methods. Flame properties were predicted using the detailed mechanisms of Refs. 5-8, see Xu et al. [1,2] for complete descriptions of methods. These predictions were obtained using the steady, laminar, one-dimensional premixed flame computer program, PREMIX, of Kee et al. [10]. PREMIX allows for mixture-averaged multi-component diffusion and variable thermophysical and transport properties. Present measurements were used to prescribe temperatures as a function of distance from the burner in order to minimize computational uncertainties due to effects of heat loss to the burner and flame radiation. Both chemical mechanisms were limited to hydrocarbons up to benzene and involved 250 reversible reactions and 52 species for the mechanism of Frenklach and coworkers [6-8] and 451 reversible reactions and 87 species for the approach of Leung and Lindstedt [5]. Finally, predictions of H concentrations were also completed similar to Refs. 1 and 2, based on measured temperature and H_2, concentrations and obtaining equilibrium constants from Kee et al. [10].

* Corresponding author, gmfaeth@umich.edu

Results and Discussion. Typical measurements of flame temperatures, T, soot volume fractions, f_v, and the mole fractions of major stable gas species are plotted as a function of distance from the burner exit,, z, in Fig. 1 for methane/oxygen flames for ϕ=2.45 and in Fig. 2 for ϕ=2.67. Present measurements are limited to the post-flame soot growth region and begin at z=5 mm. Within this region, increasing z implies decreasing T due to radiative heat losses,, increasing f_v due to soot nucleation and growth, relatively small variations of combustion products and the low level of N_2 dilution (N_2 is present because it was used as the carrier gas for introducing lithium chloride into the flame), and modest reductions of hydrocarbon (C_2H_2, CH_4, C_2H_4) concentrations. The present variations of hydrocarbons are somewhat larger and present soot concentrations are somewhat smaller than the flames studied earlier [2]. This behavior comes about because the present flames have larger flow velocities than the earlier flames in order to safely stabilize the flames on the open structured honeycomb; this extends the early stages of the soot growth region over the present test range where some hydrocarbon decomposition is still occurring. The formation of soot itself is not responsible for these changes of hydrocarbon concentrations because soot contains a very small fraction (<0.01%) of the mass of carbon in these flames. Soot concentrations are seen to be larger at ϕ=2.67 than at ϕ=2.45 (roughly twice as large). It will be seen later that H-atom concentrations are similar for these two flames; therefore, the larger acetylene concentrations of the flame having the larger fuel equivalence ratio is responsible for its larger soot concentrations through the HACA mechanism.

Predictions and measurements of major gas species concentrations as a function of ϕ are illustrated in Fig. 3. Both mechanisms yield the same results and provide excellent predictions of the major gas species concentrations, e.g., H_2, CO_2, CH_4, H_2O and CO. Predictions of C_2H_2 and C_2H_4 are qualitatively correct but somewhat less satisfactory: this behavior is generally similar to the earlier findings for methane/oxygen flames [2].

Measurements and predictions of H concentrations for flames having ϕ= 2.45, 2.56 and 2.67 are illustrated in Fig. 4. Typical of past experience [1,2], the mechanisms of [5] and [6-8] yield essentially the same results. The main reason for this is that equilibrium is maintained between H and H_2 throughout the soot growth region, as indicated by present predictions of H concentrations, while both mechanisms yield the same H_2 concentrations as noted in connection with the discussion of Fig. 3. More importantly, all these estimates agree with present measurements of H concentrations within experimental uncertainties. This provides strong support for the assumption the H_2 and H were in thermodynamic equilibrium for similar flame conditions during evaluation of HACA mechanism in Refs. 1 and 2.

Acknowledgments. This research was sponsored by NASA Grant Nos. NAG-3-1245, 1878 and 2048 under the technical management of D.L. Urban and Z.-G. Yuan of the NASA Lewis Research Center.

References.

1. Xu, F., Sunderland, P.B. and Faeth, G.M., Combust. Flame 108:471 (1997).
2. Xu, F., Lin, K.-C. and Faeth, G.M., Combust. Flame 115:195 (1998).
3. Harris, S.J. and Weiner, A.M., Combust. Sci. Tech. 31:155 (1983); ibid., 32:267 (1983); ibid., 38:75 (1984).
4. Ramer, E.R., Merklin, J.F., Sorensen, C.M. and Taylor, T.W., Combust. Sci. Tech. 48:241 (1986).
5. Leung, K.M. and Lindstedt, R.P., Combust. Flame 102:129 (1995).
6. Frenklach, M., 23rd Symposium (International) on Combustion, The Combustion Institute, Pittsburgh, 1990, p.1559.
7. Frenklach, M. and Wang, H., Soot Formation in Combustion (H. Bockhorn, ed.), Springer-Verlag, Berlin, 1994, p.165.
8. Kazakov,A., Wang, H. and Frenklach, M., Combust. Flame 100:111 (1995).
9. Colket, M.B. and Hall, R.J., Soot Formation in Combustion (H. Bockhorn, ed.), Springer-Verlag, Berlin, 1994, p.442.
10. Kee, R.J., Grcar, J.F., Smooke, M.D. and Miller, J.A., A Fortran Program for Modeling Steady Laminar One-Dimensional Premixed Flames, Report No. SAND 85-8240, Sandia National Laboratories, Albuquerque,NM, 1985.
11. Neoh, K.G., Howard, J.B. and Sarofim, A.F., Particulate Carbon (D.C. Siegla and B.W. Smith, eds.), Plenum Press, New York, 1980, p. 261.

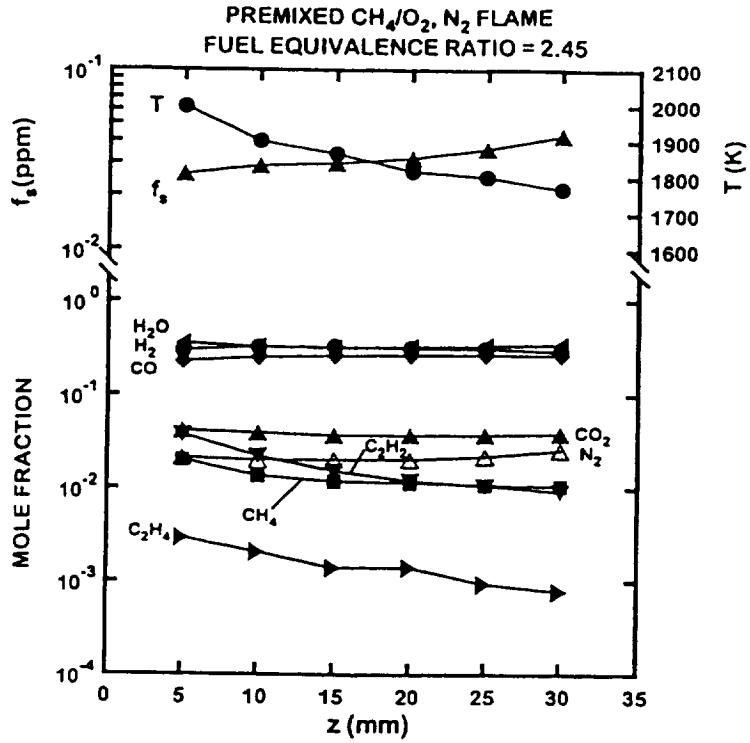

Fig. 1 Soot and flame properties along the axis of the fuel-equivalence ratio = 2.45 flame.

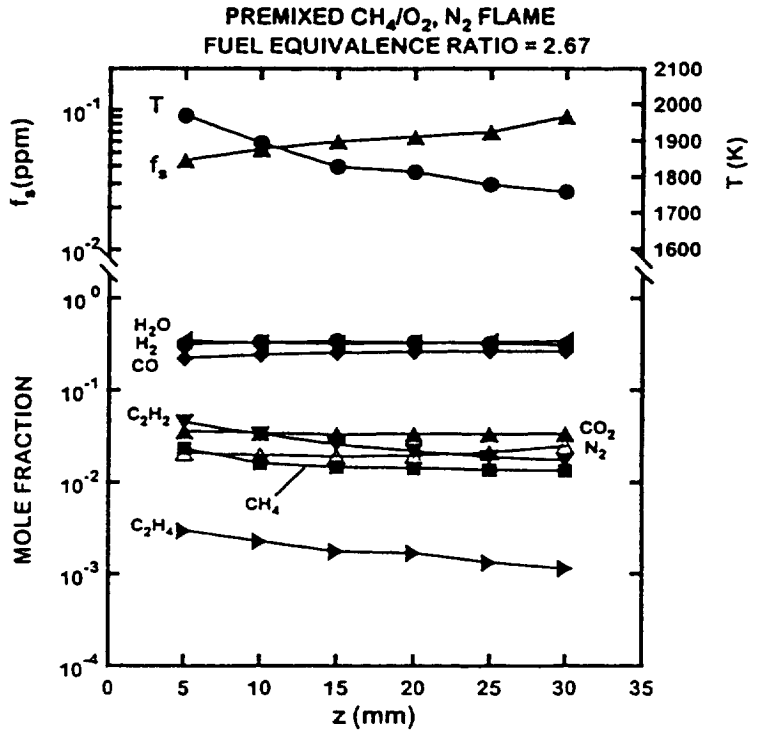

Fig. 2 Soot and flame properties along the axis of the fuel-equivalence ratio =2.67 flame.

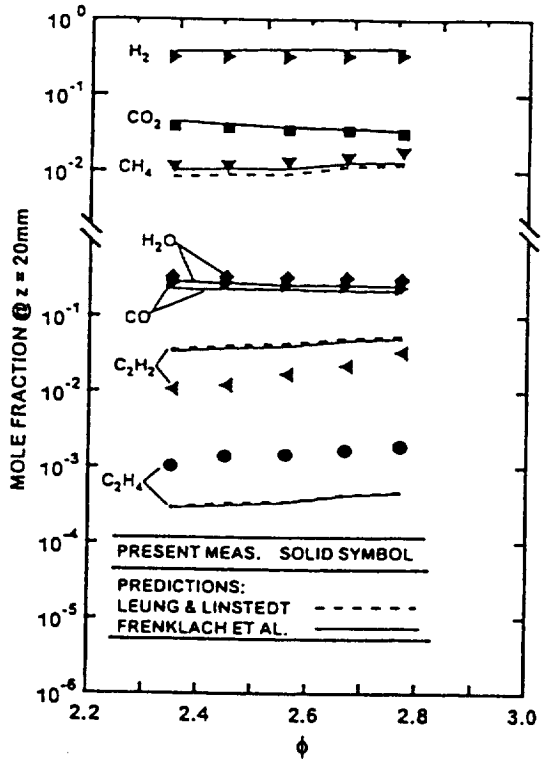

Fig. 3 Measured and predicted concentrations of major gas species at the axis of the present flames at z = 20 mm. Predictions based on the mechanisms of Leung and Lindstedt [5] and Frenklach et al. [6-8].

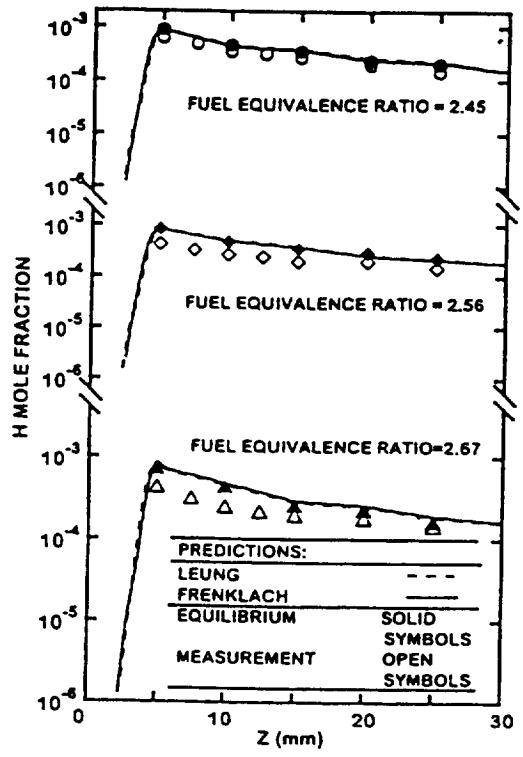

Fig. 4 Measured and predicted H-atom concentrations along the axis of the present flames. Predictions based on the mechanisms of Leung and Lindstedt [5] and Frenklach et al. [6-8] and the assumption of local thermodynamic equilibrium using equilibrium constants from Kee et al. [10].